Glutarate metabolism in *Pseudomonas putida* is regulated by two distinct glutarate sensing transcription factors

Mitchell G. Thompson[1,2,3], Pablo Cruz-Morales[1,2,4], Rohith N. Krishna[1,2,5],Jacquelyn M. Blake-Hedges[1,2,5], Matthew R. Incha[1,2,3], Jay D. Keasling[1,2,6,7,8]

[1]Joint BioEnergy Institute, 5885 Hollis Street, Emeryville, CA 94608, USA.

[2]Biological Systems & Engineering Division, Lawrence Berkeley National Laboratory, Berkeley, CA 94720, USA.

[3]Department of Plant and Microbial Biology, University of California, Berkeley, CA 94720, USA

[4]Centro de Biotecnologia FEMSA, Instituto Tecnologico y de Estudios superiores de Monterrey, Mexico

[5]Department of Chemistry, University of California, Berkeley, CA 94720, USA

[6]Joint Program in Bioengineering, University of California, Berkeley/San Francisco, CA 94720, USA

[7]Department of Chemical and Biomolecular Engineering, University of California, Berkeley, CA 94720, USA

[8]The Novo Nordisk Foundation Center for Biosustainability, Technical University of Denmark, Denmark

ABSTRACT

Transcription factor based biosensors can be leveraged to screen thousands of genetics designs for optimal production in engineered microbes. In this study we characterize two glutarate sensing transcription factors (CsiR and GcdR) from *Pseudomonas putida*. The genomic contexts of CsiR homologs were analyzed and DNA binding sites were bioinformatically predicted. Both CsiR and GcdR were purified and shown to bind upstream of their coding sequencing *in vitro*. CsiR was shown to dissociate from DNA *in vitro* when exogenous glutarate was added confirming it acts as a genetic repressor. Both transcription factors were then engineered into plasmid based biosensors and their respective sensing performance features calculated. Both sensor plasmids were then reintroduced into *P. putida* and were evaluated for their ability to sense flux through glutarate when grown on various lysine metabolites as sole carbon sources. These findings provide information describing glutarate flux in *P. putida*, and potentially useful tools for future metabolic engineering and synthetic biology efforts.

INTRODUCTION

A rate limiting step in the design, build, test cycle is often the test phase, wherein hundreds or thousands of genetic designs need to be evaluated for their productivity [1,2]. Though recent advances in analytical chemistry have dramatically increased sample throughput [3], transcription factor based biosensors still offer multiple advantages over traditional chromatographic and mass-spectrometry based detection methods. One of the most attractive benefits is the ability to rapidly screen constructs for the production of the target compounds via either plate based, or flow-cytometry based assays [1–3]. Additionally, biosensors may offer unmatched sensitivity towards specific ligands, with some sensors having picomolar affinity [3].

The evolution of diverse microbial metabolism has provided researchers with a wide array of ligands capable of being sensed, ranging from complex natural products [4,5], to small central metabolites [1,6].

Work in our lab has developed biosensors to detect multiple lactams [6], which can be utilized to synthesize economically important polymers such as nylon [7]. These polymers also require diacids, such as adipic acid, for their polymerization. The L-lysine metabolism of *Pseudomonas putida* has been leveraged to produce the omega-amino acid 5-aminovaleric acid (5AVA), as well as the diacid glutarate [7,8]. Recently it has been found that glutarate metabolism in *P. putida* can be degraded either by a ketogenic route to acetyl-coA or through a glucogenic route to succinate [8] (Figure 1). Work in our lab has also shown this metabolism, and demonstrated that both glutarate catabolic pathways are highly upregulated in the presence of glutarate [9]. While work in *Pseudomonas aeruginosa* has characterized a homolog of the regulator of the ketogenic pathway (GcdR) [10], and work in *Escherichia coli* has preliminarily characterized the glucogenic pathway regulator (CsiR), no work has directly investigated the regulation of the *P. putida* L-lysine catabolic pathways.

In this work we sought to better characterize the two putative local regulators of glutarate catabolism in *P. putida*, *csiR* and *gcdR*. First, we compared the genomic context of *csiR* homolongs across bacteria, to bioinformatically predict a conserved DNA binding site. We then biochemically, and genetically characterized both regulators. Finally we introduced RFP transcriptional fusions of the promoter for both catabolic pathways into *P. putida* and evaluated their induction upon the addition of various lysine metabolites.

RESULTS

Genomic Contexts of CsiR and GcdR Homologs and Prediction of *P. putida* binding sites

Work in *Pseudomonas aeruginosa* has characterized the GcdR regulation of ketogenic glutarate metabolism, and shown that the binding site is conserved across multiple bacterial species [10]. While binding sites for CsiR in *E. coli* have been identified, whether there is a conserved binding site for homologs across bacterial species has yet to be investigated [11]. In order to identify conserved binding sites of CsiR homologs, 19 selected genomes that contained neighboring CsiD and CsiR homologs had their syntenic genomic contexts compared. Genes encoding *csiR* were found in two distinct genomic contexts, either transcribed divergently from *csiD* as found in *P. putida*, or transcribed as the last gene in the *csi* operon as in *E. coli* (Figure 2). The genomic regions upstream of the *csiD* homolog were extracted and MEME was used to identify a conserved CsiR binding motif. A consensus A(A/G)AAATCTAGA(C/T)ATTTT motif was identified upstream of each *csiD* homolog. Previously, footprinting assays in *E. coli* revealed two primary and two secondary bindings sites with the sequences TTGTN$_5$TTTT and ATGTN$_5$TTTT respectively [11]. Our consensus motif agrees closely with the secondary binding site identified, and highly suggests that the binding site of CsiR is conserved across the bacteria where homologs are present.

<u>Biochemical characterization of CsiR and GcdR</u>

To determine if the *P. putida* CsiR also acts as a regulator and to identify its putative binding sites, we biochemically characterized this protein using electrophoretic mobility shift assays (EMSAs). The CsiR protein was purified and incubated with DNA probes consisting of the intergenic region between *csiR* and *csiD*. The assay showed multiple binding sites in this intergenic region, as four distinct bands appeared. These results appear to confirm the finding in *E. coli* where four binding sites of the *E. coli* CsiR homolog were observed [11]. CsiR demonstrated a high affinity for the DNA probe, with a calculated K_d of approximately 30 nM

(Figure 3a), which is similar to the CsiR/DNA K_d of the *E. coli* CsiR homolog which was determined to be 10nM [11]. GcdR also bound to its cognate probe, with a single distinct shift, with an estimated K_d of approximately 62.5 nM (Figure 3a) [10]. As CsiR is a GntR family transcriptional regulator, many of which act as repressors [12], we evaluated whether glutarate would decrease the DNA binding affinity of CsiR. EMSA assays were repeated in the presence of increasing glutarate concentrations. Analysis by gel electrophoresis revealed increasing quantities of free probe as glutarate concentrations increased (Figure 3b). These results confirm that the *P. putida* CsiR is a glutarate-responsive repressor of the *csiDlhgO* operon.

Development of two glutarate biosensor vectors

In order to evaluate both CsiR and GcdR as biosensors we cloned both the regulator and intergenic region of both the ketogenic and glucogenic glutarate catabolism pathways upstream of RFP on a broad host range plasmid (Figure 4a). *E. coli* harboring either plasmid were grown for 24 hours in LB supplemented with concentrations of glutarate ranging from 50 mM to 6.1 uM, after which both OD600 and RFP fluorescence were measured. At concentrations above 6.25 mM glutarate proved to be toxic to cells, and RFP measurements from these concentrations were not used to calculate biosensor performance features (Figure 4b). The CsiR reporter vector had significantly higher background than the GcdR vector, indicating leakier expression (Figure 4b). Normalized RFP expression data was then fit to the Hill equation to derive biosensor performance (Figure 4c). Both sensors showed similar linear ranges (0.05 - 3.13 mM for CsiR, and 0.05 - 6.25 mM for GcdR), however the K_m for CsiR was lower than GcdR (0.65 mM versus 2.24 mM). The GcdR reporter displayed greater sensitivity than the CsiR vector (Hill coefficient of 1.09 versus 0.75), in addition to a greater maximum expression of RFP (65000 versus 42000).

Responsiveness of Glutarate Biosensors to Lysine metabolites in *P. putida*

To evaluate the ability of both reporter vectors to monitor glutarate flux *in vivo*, both plasmids were introduced into wild-type *P. putida* KT2440 and grown on L-lysine and D-lysine metabolites as sole carbon sources. Both strains were grown on 10 mM Glucose, L-lysine, D-lysine, 5-aminovalerate, or 2-aminoadipatefor 48 hours with OD_{600} and RFP fluorescence being measured continuously (Figures 5a and 5b). Neither reporter was induced when the bacterium was grown on glucose (Figure 5b). The GcdR reporter was strongly induced by 5-aminovaleate, and to a less extent 2-aminoadipate, D-lysine, and L-lysine (Figure 5b). Conversely, the strain harboring the CsiR reporter plasmid only displayed r induction of RFP above background only when grown on 5-aminovalerate. While 5-aminovalerate was able to induce RFP induction in the strain harboring the CsiR reporter, induction was extremely limited compared to induction of RFP from the GcdR reporter vector (Figure 5b).

DISCUSSION

Recent advances in high-throughput functional genomics have allowed researchers to rapidly identify novel metabolic pathways, and in turn infer the function of novel transcription factors [13,14]. Rigorous characterization of these regulators is a critical step to developing novel parts for synthetic biology, as well as useful tools for metabolic engineering. The discovery of two distinct pathways for glutarate catabolism within *P. putida*, regulated by independent transcription factors, presents an interesting opportunity to compare and contrast the relative sensing properties of each system.

The *P. aeruginosa* GcdR was demonstrated to be a positive regulator of the *gcdHG* operon, with a binding site that was conserved in *P. putida* KT2440 among other *Pseudomonas* strains [10]. While other strains of *P. aeruginosa* have *csiD* homologs, the type strain PA01 does not. However, *csiDlghO* pathways have been rigorously characterized in both *P. putida* and *E.*

coli, though only in *E. coli* has the CsiR homolog been characterized [8,9,11]. Our bioinformatic approach to predict the conserved binding site of CsiR largely agrees with the empirically determined binding site identified in *E. coli*, and our EMSA results also confirm the existence of four distinct CsiR binding sites. The dissociation of CsiR from the DNA probe with the addition of glutarate *in vitro* verifies that CsiR is a negative regulator of CsiD, which is expected as many GntR-type regulator tend to act as repressors. The existence of a primary and secondary series of binding sites suggests a canonical autoregulatory negative feedback loop, found in an estimated ~60-70% of bacterial transcription factors [15]. Further work will need to be done to characterize any such autoregulation.

Plasmid-based biosensors of both the CsiR and GcdR systems displayed low uM limits of detection in *E. coli*. While the CsiR biosensor displayed greater sensitivity to glutarate at lower inducer concentrations, its maximum output was considerably less than the GcdR system and saturated at low mM concentrations of glutarate. Furthermore the CsiR system showed substantially higher background RFP than the GcdR based system. While the CsiR system may be useful for detecting low concentrations of glutarate, further engineering will need to be done to increase its utility. GcdR displayed a larger linear range of detection, and a greater maximal output that the CsiR system, in addition to a relatively low level of background expression. These properties may make the GcdR system more attractive as a glutarate biosensor. Furthermore, given that glutarate is relatively inexpensive, the GcdR system may make an excellent inducible expression system. Further work will need to be conducted to evaluate the utility of the GcdR expression system in other bacteria.

In addition to their utility as biosensors for metabolic engineering, these sensors are a valuable tool in studying the carbon flux in the native host *P. putida*. Lysine metabolism in *P.*

putida is isomer specific, with each isomer being degraded by a separate catabolic pathway [9]. While cross-feeding between the pathways has been proposed previously [16], recent work by our group has proposed a molecular mechanism for metabolite exchange between the D- and L-catabolic pathways [9]. The exchange relies on the 2-oxoacid promiscuity of the non-heme Fe(II) oxidase CsiD which normally catalyzes the hydroxylation of glutarate using 2-ketoglutarate as a cosubstrate to yield 2-hydroxyglutarate and succinate. CsiD can also use 2-oxoadipate, a D-lysine catabolic intermediate, as a 2-oxoacid cosubstrate to yield 2-hydroxyglutarate and glutarate as products. The glutarate from this reaction could then proceed down the L-lysine catabolic pathway. When 2-aminoadipate was fed into *P. putida* harboring the GcdR reporter, fluorescence was observed in stationary phase. As 2-aminoadipate immediately precedes 2-oxoadipate in the D-lysine catabolic pathway, these results support the hypothesis that CsiD could act as a bridge between the two catabolic pathways.

There has been substantial interest in developing microbes to produce glutarate, with strains of *E. coli*, *P. putida*, and *Corynebacterium glutamicum* all engineered to produce high titers [8,17,18]. Further engineering of the GcdR system may be able to extend the linear range to higher concentrations furthering its utility as a tool to achieve even higher titers of glutarate. Though glutarate is a valuable commodity chemical, the C6 diacid adipate is used in much greater quantities primarily as a monomer used to make nylons [19]. Recent work has readily demonstrated the means to evolve transcription factors to sense non-native ligands [4]. Such methods could be applied to either CsiR or GcdR in order to expand their utility in sensing other industrially important diacids.

METHODS

Media, chemicals, and culture conditions

General *E. coli* cultures were grown in Luria-Bertani (LB) Miller medium (BD Biosciences, USA) at 37 °C while *P. putida* was grown at 30 °C. When indicated, *P. putida* and *E. coli* were grown on modified MOPS minimal medium [20]. Cultures were supplemented with kanamycin (50 mg/L, Sigma Aldrich, USA), gentamicin (30 mg/L, Fisher Scientific, USA), or carbenicillin (100mg/L, Sigma Aldrich, USA), when indicated. All other compounds were purchased through Sigma Aldrich (Sigma Aldrich, USA) .

Strains and plasmids

All bacterial strains and plasmids used in this work are listed in Table 1. All strains and plasmids created in this work are available through the public instance of the JBEI registry. (https://public-registry.jbei.org/folders/390). All plasmids were designed using Device Editor and Vector Editor software, while all primers used for the construction of plasmids were designed using j5 software [21–23]. Plasmids were assembled via Gibson Assembly using standard protocols [24], or Golden Gate Assembly using standard protocols [25]. Plasmids were routinely isolated using the Qiaprep Spin Miniprep kit (Qiagen, USA), and all primers were purchased from Integrated DNA Technologies (IDT, Coralville, IA).

Expression and purification of proteins

Proteins were purified as described previously [26]. Briefly, a 500 mL cultures of *E. coli* BL21 (DE3) harboring expression plasmids were grown on LB media at 37 ºC to an OD of 0.6 then induced with 1mM Isopropyl β-D-1-thiogalactopyranoside Cells were allowed to express for 18 hours at 30 ºC before being harvested via centrifugation. Cell pellets were stored at -80 ºC until purification. Cell pellets were then resuspended in lysis buffer (50 mM sodium phosphate, 300 mM sodium chloride, 10 mM imidazole, 8% glycerol, pH 7.5) and sonicated to lyse cells. Insolubles were pelleted via centrifugation (30 minutes at 40,000xg). The supernatant

was applied to a fritted column containing Ni-NTA resin (Qiagen, USA) which had been pre-equilibrated with several column volumes of lysis buffer. The resin was washed with lysis buffer containing 50 mM imidazole, then the protein was eluted using a step-wise gradient of lysis buffer containing increasing imidazole concentrations (100 mM, 200 mM, and 400 mM). Fractions were collected and analyzed via SDS-PAGE. Purified proteins were concentrated using Spin-X UF 20 (10 kDa MWCO) spin concentrators (Corning, Inc.). Concentrated protein was stored at 4 ºC until *in vitro* analysis.

Plate based growth and fluorescence assays

Growth studies of bacterial strains were conducted a microplate reader kinetic assays. Overnight cultures were inoculated into 10 mL of LB medium from single colonies, and grown at 30 °C. These cultures were then washed twice with MOPS minimal media without any added carbon and diluted 1:100 into 500 uL of MOPS medium with 10 mM of a carbon source in 48-well plates (Falcon, 353072). Plates were sealed with a gas-permeable microplate adhesive film (VWR, USA), and then optical density and fluorescence were monitored for 48 hours in an Biotek Synergy 4 plate reader (BioTek, USA) at 30 °C with fast continuous shaking. Optical density was measured at 600 nm, while fluorescence was measured using an excitation wavelength of 561 nm and an emission wavelength of 605 nm with a manually set gain of 100.

Transcriptional fusion fluorescence assays

To measure RFP production from *E. coli* reporter plasmids, fluorescence measurements were obtained from single time points of cells grown in deep-well 96-well plates as described previously [27]. Briefly Cells were grown in 500 µL of LB medium supplemented with kanamycin and a range of glutarate concentrations from 5 mM to 0 mM. Plates were sealed with AeraSeal film (Excel Scientific, AC1201-02) and grown for 22 hours at 30 °C on a 200 rpm

shaker rack. After incubation, 100 µL from each well was aliquoted into a black, clear-bottom 96-well plate and fluorescence was measured with an Infinite F200 Pro (Tecan Life Sciences, San Jose, CA) plate reader. Optical density was measured at 600 nm, while fluorescence was measured using an excitation wavelength of 575 nm and an emission wavelength of 620 nm with a manually set gain of 85.

Electrophoretic mobility shift assays

Electrophoretic mobility shift assays were performed as previously described [5]. 6-Carboxyfluorescein labelled PCR products to generate probes for CsiR were generated from the intergenic region between PP_2908 and PP_2909 using primers csiRprobeFOR 5'-6-FAM/AGTTCGATCTGCGTAAAG-3' and csiRprobeREV 5'-CCCGCTGAATGCTGAGTT-3'), while probes for GcdR were generated from the intergenic region between PP_0157 and PP_0158 with primers gcdRprobeFOR 5'-6-FAM/CGGGTCGATCCAGTTGAAA-3' and gcdRprobeREV 5'-GCATGTACGTCAACCTCACT-3'. Primers were purchased from IDT Technologies (IDT, Coralville, IA). PCR product was then purified with a QIAquick PCR Purification Kit (Qiagen, USA), and the amount of DNA was quantified via a NanoDrop 2000C (There Fisher Scientific). Binding reactions were conducted with 10 ng of labelled probe, which was added to 10 mM Tris–HCl (pH 8.0), 25 mM KCl, 2.5 mM MgCl2, 1.0 mM DTT and 2 ug salmon sperm DNA in 20 uL reactions. CsiR was added to reactions in concentrations ranging from 250 nM to ~4 nM in addition to no CsiR controls, and then allowed to incubate at 22 ºC for 20 minutes. Reactions were then loaded into 10% native polyacrylamide gels buffered with 0.5x TBE. After electrophoresis gels were imaged on a Alpha Innotech MultiImage III (Alpha Innotech). Pixel intensity to estimate K_d was done in Adobe Photoshop.

Bionformatic Analysis and Analysis of Biosensor Parameters

Biosensing parameters were calculated as previously described [1]. For the phylogenetic reconstructions, the best amino acid substitution model was selected using ModelFinder as implemented on IQ-tree [28] phylogenetic trees were constructed using IQ-tree, nodes were supported with 10,000 bootstrap replicates. The final tree figures were edited using FigTree v1.4.3 (http://tree.bio.ed.ac.uk/software/figtree/). Orthologous syntenic regions of CsiR were identified with CORASON-BGC [29] and manually colored and annotated. DNA-binding sites were predicted with MEME [30].

Acknowledgements

Python code to analyze biosensor performance characteristics was partially written by Dr. Zak Costello. The authors would like to thank the UC Berkeley SMART program for providing support for R.K to conduct summer research. This work was part of the DOE Joint BioEnergy Institute (https://www.jbei.org) supported by the U.S. Department of Energy, Office of Science, Office of Biological and Environmental Research. The views and opinions of the authors expressed herein do not necessarily state or reflect those of the United States Government or any agency thereof. Neither the United States Government nor any agency thereof, nor any of their employees, makes any warranty, expressed or implied, or assumes any legal liability or responsibility for the accuracy, completeness, or usefulness of any information, apparatus, product, or process disclosed, or represents that its use would not infringe privately owned rights.

Contributions

Conceptualization, M.G.T.; Methodology, M.G.T., J.M.B, P.C.M.; Investigation, M.G.T., J.M.B, R.N.K, P.C.M, M.R.I..; Writing – Original Draft, M.G.T, M.R.I..; Writing – Review and Editing, All authors.; Resources and supervision, J.D.K.

Competing Interests

J.D.K. has financial interests in Amyris, Lygos, Constructive Biology, Demetrix, Napigen and Maple Bio.

Figure Legends

Figure 1: Organization of the two routes of glutarate metabolism in *P. putida*.

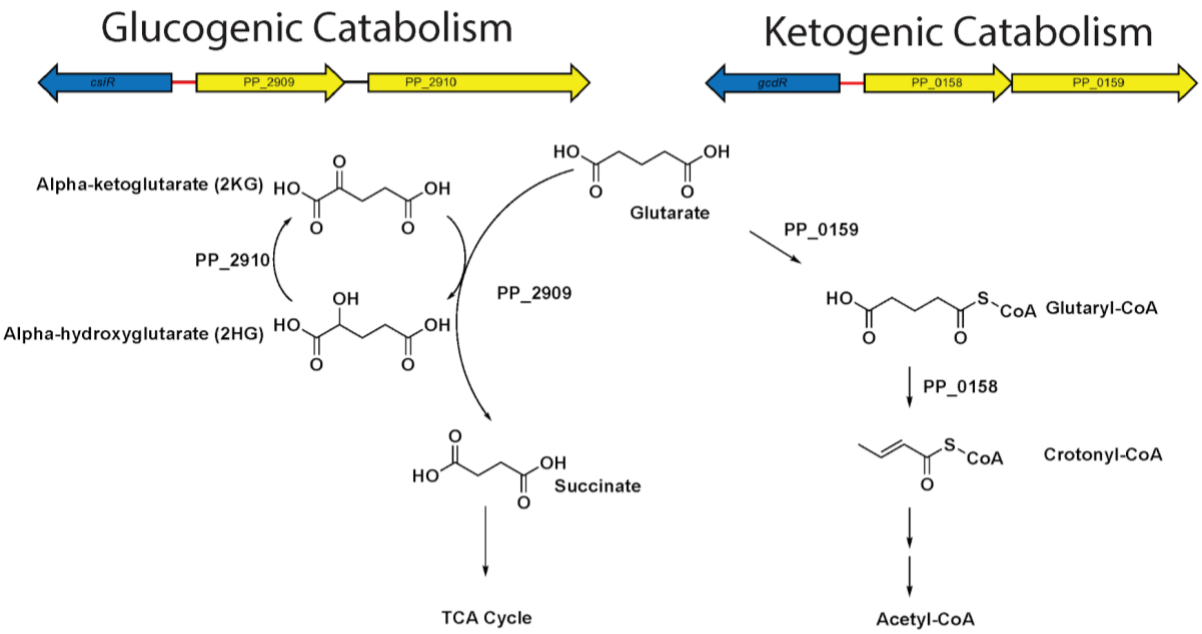

Figure 2: Genomic contexts of CsiR homologs and predicted binding regions: Phylogeny of assorted gammaproteobacteria and the location of their *csiD* operons. MEME analysis of the

intergenic regions upstream of the *csiD* operon resulted in the sequence motifs depicted below the tree.

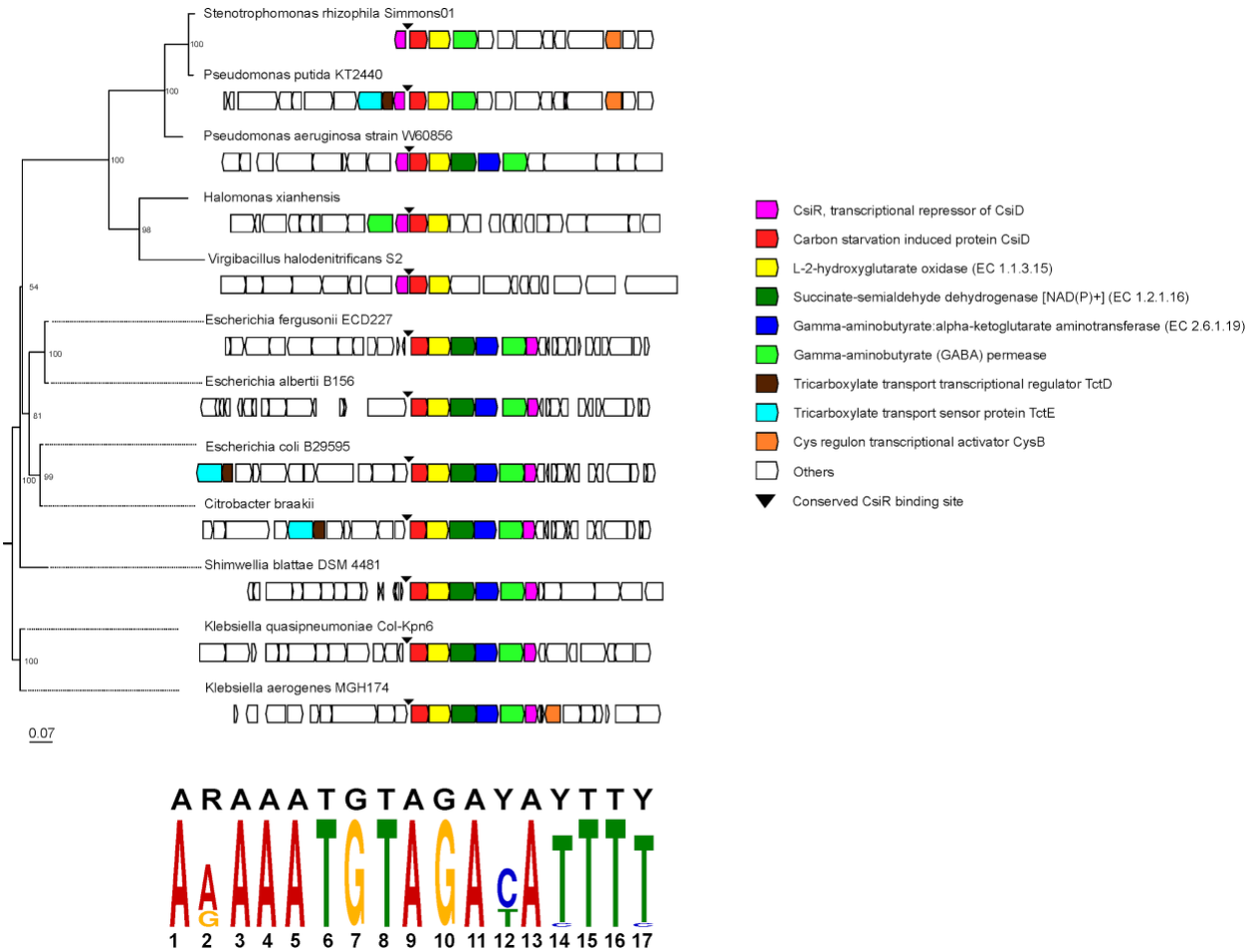

Figure 3: Biochemical characterization of CsiR and GcdR. (A) EMSA of either purified CsiR (left) or GcdR (right) incubated with fluorescent probe of intergenic region between *csiR* and *csiD*. Concentrations of CsiR protein range from 0nM to 250nM. (B) EMSA showing 100nM CsiR and fluorescent probe incubated with glutarate from concentrations of 0 mM to 5 mM. Far left lane shows free probe with no CsiR.

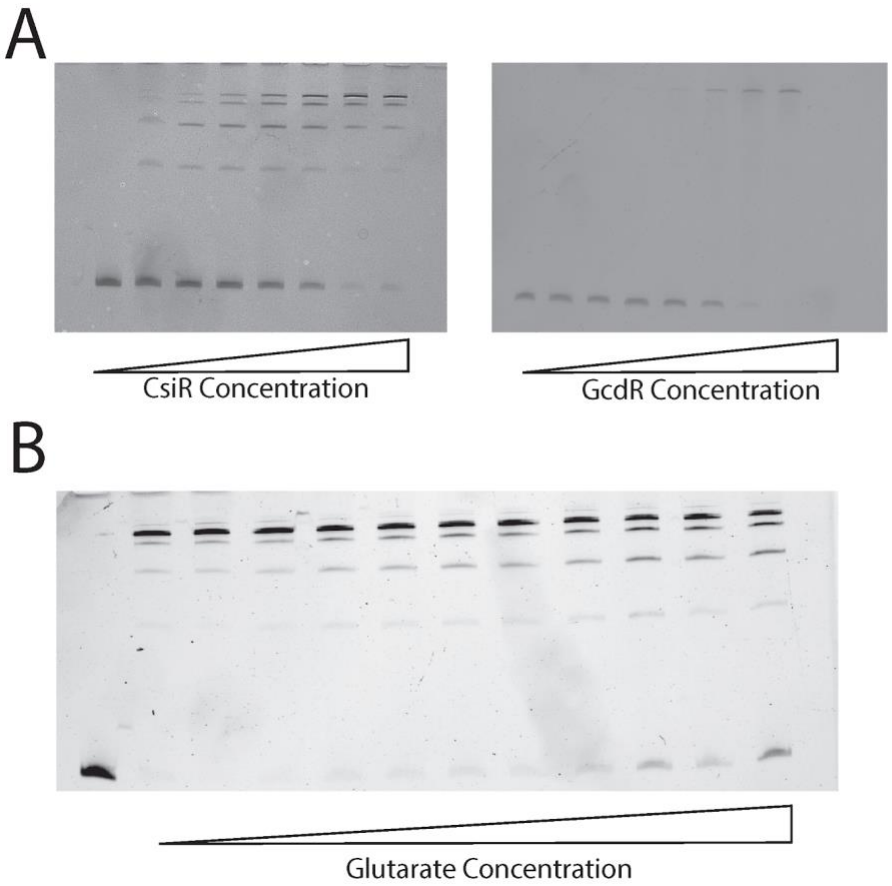

Figure 4: Developing glutarate responsive reporter vectors for *E. coli*. (A) Plasmid designs for glutarate responsive vectors (B) Fluorescence measured from either a CsiR (left) or GcdR (right) transcriptional reporter in *E. coli*. Bars show fluorescence measured in arbitrary units normalized to OD_{600} in response to mM concentrations of glutarate. Error bars show 95% CI, n=4. (C) Fluorescence data fit to the Hill equation to derive biosensor performance characteristics. Table below fitted data summarizes relevant biosensor features.

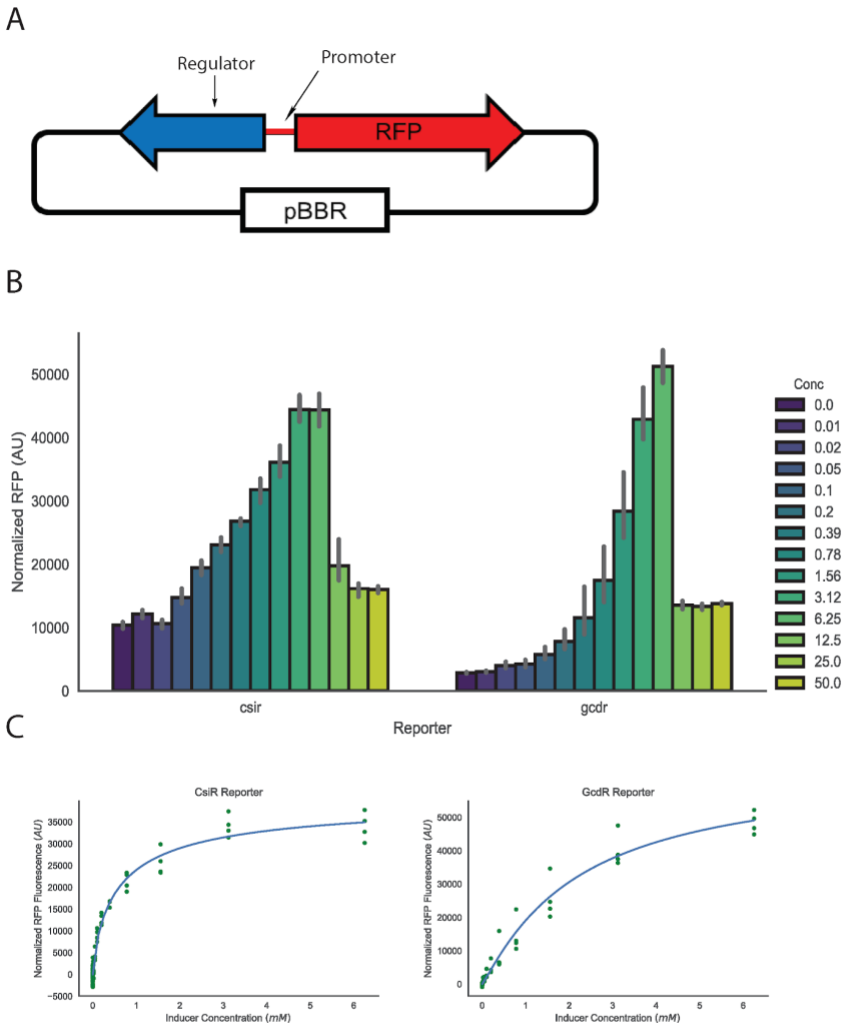

Sensor	RFPmax	Km (mM)	Hill Coefficient	Linear Range (mM)
CsiR	42000	0.65	0.75	0.05-3.13
GcdR	65000	2.24	1.09	0.05-6.25

Figure 5: Growth and fluorescence of PcsiD and PgcdH reporter in P. putida KT2440 (A) Growth of strains harboring gcdR reporter (left), or csiR reporter (right) on MOPS minimal media supplemented with 10mM of glucose, L-lysine, D-lysine, 5-aminovalerate, or 2-aminoadipate as a sole carbon source. Shaded region represents 95% CI, n=3. (B) RFP fluorescence of strains harboring gcdR reporter (left), or csiR reporter (right) on MOPS minimal

media supplemented with 10mM of glucose, L-lysine, D-lysine, 5-aminovalerate, or 2-aminoadipate as a sole carbon source. Shaded region represents 95% CI, n=3.

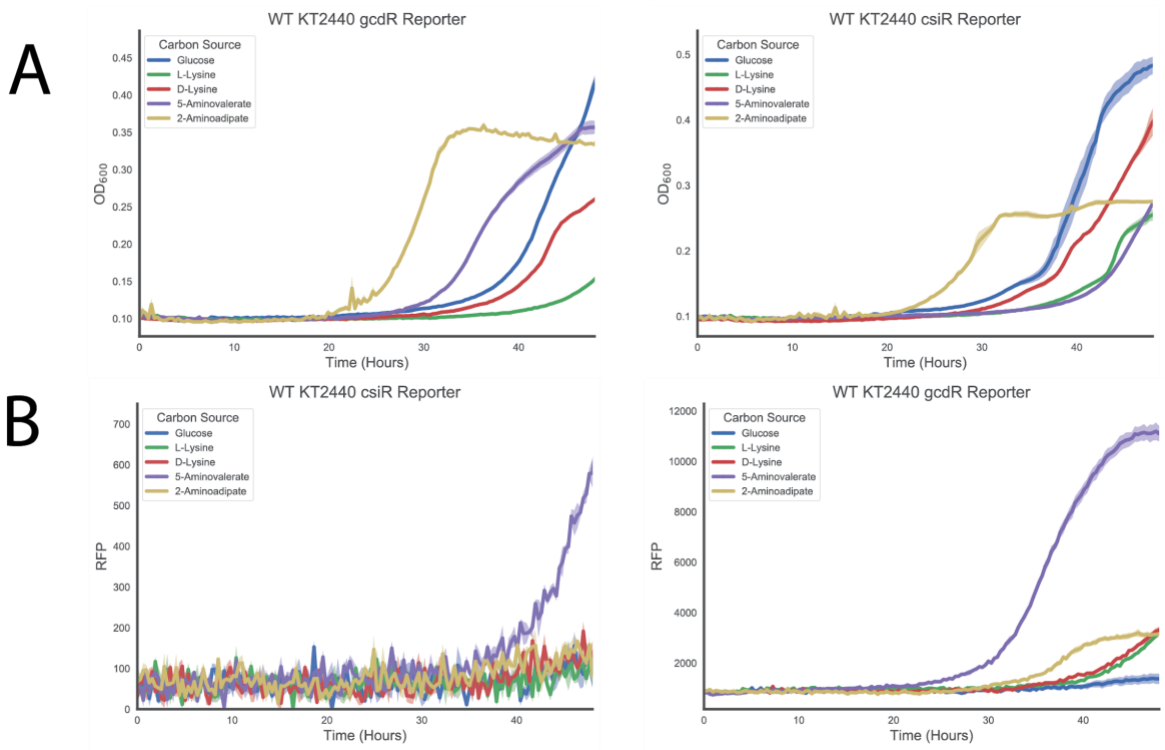

Table 1.

Strain	JBEI Part ID	Reference
E. coli DH10B		[31]
E. coli BL21(DE3)		Novagen
P. putida KT2440		ATCC 47054
Plasmids		

pET21b		Novagen
pBADT		[32]
pBADT-gcdR-PgcdH::RFP	JPUB_010960	This work
pBADT-csiR-PcsiD::RFP	JPUB_010962	This work
pET21b-CsiR_Pput	JPUB_010964	This work
pET21b-GcdR_Pput	JPUB_010966	This work

Bibliography

1. Dietrich JA, Shis DL, Alikhani A, Keasling JD. Transcription factor-based screens and synthetic selections for microbial small-molecule biosynthesis. ACS Synth Biol. 2013;2: 47–58. doi:10.1021/sb300091d

2. Dietrich JA, McKee AE, Keasling JD. High-throughput metabolic engineering: advances in small-molecule screening and selection. Annu Rev Biochem. 2010;79: 563–590. doi:10.1146/annurev-biochem-062608-095938

3. Petzold CJ, Chan LJG, Nhan M, Adams PD. Analytics for metabolic engineering. Front Bioeng Biotechnol. 2015;3: 135. doi:10.3389/fbioe.2015.00135

4. Kasey CM, Zerrad M, Li Y, Cropp TA, Williams GJ. Development of Transcription Factor-Based Designer Macrolide Biosensors for Metabolic Engineering and Synthetic Biology. ACS Synth Biol. 2018;7: 227–239. doi:10.1021/acssynbio.7b00287

5. Lei C, Wang J, Liu Y, Liu X, Zhao G, Wang J. A feedback regulatory model for RifQ-mediated repression of rifamycin export in Amycolatopsis mediterranei. Microb Cell Fact. 2018;17: 14. doi:10.1186/s12934-018-0863-5

6. Zhang J, Barajas JF, Burdu M, Ruegg TL, Dias B, Keasling JD. Development of a Transcription Factor-Based Lactam Biosensor. ACS Synth Biol. 2017;6: 439–445. doi:10.1021/acssynbio.6b00136

7. Zhang J, Barajas JF, Burdu M, Wang G, Baidoo EE, Keasling JD. Application of an Acyl-

CoA Ligase from Streptomyces aizunensis for Lactam Biosynthesis. ACS Synth Biol. 2017;6: 884–890. doi:10.1021/acssynbio.6b00372

8. Zhang M, Gao C, Guo X, Guo S, Kang Z, Xiao D, et al. Increased glutarate production by blocking the glutaryl-CoA dehydrogenation pathway and a catabolic pathway involving L-2-hydroxyglutarate. Nat Commun. 2018;9: 2114. doi:10.1038/s41467-018-04513-0

9. Thompson MG, Blake-Hedges JM, Cruz-Morales P, Barajas JF, Curran SC, Harris NC, et al. Massively parallel fitness profiling reveals multiple novel enzymes in Pseudomonas putida lysine metabolism. BioRxiv. 2018; doi:10.1101/450254

10. Madhuri Indurthi S, Chou H-T, Lu C-D. Molecular characterization of lysR-lysXE, gcdR-gcdHG and amaR-amaAB operons for lysine export and catabolism: a comprehensive lysine catabolic network in Pseudomonas aeruginosa PAO1. Microbiology (Reading, Engl). 2016;162: 876–888. doi:10.1099/mic.0.000277

11. Knorr S, Sinn M, Galetskiy D, Williams RM, Wang C, Müller N, et al. Widespread bacterial lysine degradation proceeding via glutarate and L-2-hydroxyglutarate. Nat Commun. 2018;9: 5071. doi:10.1038/s41467-018-07563-6

12. Jain D. Allosteric control of transcription in GntR family of transcription regulators: A structural overview. IUBMB Life. 2015;67: 556–563. doi:10.1002/iub.1401

13. Price MN, Wetmore KM, Waters RJ, Callaghan M, Ray J, Liu H, et al. Mutant phenotypes for thousands of bacterial genes of unknown function. Nature. 2018;557: 503–509. doi:10.1038/s41586-018-0124-0

14. Sagawa S, Price MN, Deutschbauer AM, Arkin AP. Validating regulatory predictions from diverse bacteria with mutant fitness data. PLoS ONE. 2017;12: e0178258. doi:10.1371/journal.pone.0178258

15. Suvorova IA, Korostelev YD, Gelfand MS. GntR Family of Bacterial Transcription Factors and Their DNA Binding Motifs: Structure, Positioning and Co-Evolution. PLoS ONE. 2015;10: e0132618. doi:10.1371/journal.pone.0132618

16. Revelles O, Espinosa-Urgel M, Molin S, Ramos JL. The davDT operon of Pseudomonas putida, involved in lysine catabolism, is induced in response to the pathway intermediate delta-aminovaleric acid. J Bacteriol. 2004;186: 3439–3446. doi:10.1128/JB.186.11.3439-3446.2004

17. Park SJ, Kim EY, Noh W, Park HM, Oh YH, Lee SH, et al. Metabolic engineering of Escherichia coli for the production of 5-aminovalerate and glutarate as C5 platform chemicals. Metab Eng. 2013;16: 42–47. doi:10.1016/j.ymben.2012.11.011

18. Rohles CM, Gießelmann G, Kohlstedt M, Wittmann C, Becker J. Systems metabolic engineering of Corynebacterium glutamicum for the production of the carbon-5 platform chemicals 5-aminovalerate and glutarate. Microb Cell Fact. 2016;15: 154.

doi:10.1186/s12934-016-0553-0

19. Hagen A, Poust S, Rond T de, Fortman JL, Katz L, Petzold CJ, et al. Engineering a polyketide synthase for in vitro production of adipic acid. ACS Synth Biol. 2016;5: 21–27. doi:10.1021/acssynbio.5b00153

20. LaBauve AE, Wargo MJ. Growth and laboratory maintenance of Pseudomonas aeruginosa. Curr Protoc Microbiol. 2012;Chapter 6: Unit 6E.1. doi:10.1002/9780471729259.mc06e01s25

21. Ham TS, Dmytriv Z, Plahar H, Chen J, Hillson NJ, Keasling JD. Design, implementation and practice of JBEI-ICE: an open source biological part registry platform and tools. Nucleic Acids Res. 2012;40: e141. doi:10.1093/nar/gks531

22. Chen J, Densmore D, Ham TS, Keasling JD, Hillson NJ. DeviceEditor visual biological CAD canvas. J Biol Eng. 2012;6: 1. doi:10.1186/1754-1611-6-1

23. Hillson NJ, Rosengarten RD, Keasling JD. j5 DNA assembly design automation software. ACS Synth Biol. 2012;1: 14–21. doi:10.1021/sb2000116

24. Gibson DG, Young L, Chuang R-Y, Venter JC, Hutchison CA, Smith HO. Enzymatic assembly of DNA molecules up to several hundred kilobases. Nat Methods. 2009;6: 343–345. doi:10.1038/nmeth.1318

25. Engler C, Kandzia R, Marillonnet S. A one pot, one step, precision cloning method with high throughput capability. PLoS ONE. 2008;3: e3647. doi:10.1371/journal.pone.0003647

26. Jackson DR, Tu SS, Nguyen M, Barajas JF, Schaub AJ, Krug D, et al. Structural Insights into Anthranilate Priming during Type II Polyketide Biosynthesis. ACS Chem Biol. 2016;11: 95–103. doi:10.1021/acschembio.5b00500

27. Thompson MG, Sedaghatian N, Barajas JF, Wehrs M, Bailey CB, Kaplan N, et al. Isolation and characterization of novel mutations in the pSC101 origin that increase copy number. Sci Rep. 2018;8: 1590. doi:10.1038/s41598-018-20016-w

28. Kalyaanamoorthy S, Minh BQ, Wong TKF, von Haeseler A, Jermiin LS. ModelFinder: fast model selection for accurate phylogenetic estimates. Nat Methods. 2017;14: 587–589. doi:10.1038/nmeth.4285

29. Cruz-Morales P, Ramos-Aboites HE, Licona-Cassani C, Selem-Mójica N, Mejía-Ponce PM, Souza-Saldívar V, et al. Actinobacteria phylogenomics, selective isolation from an iron oligotrophic environment and siderophore functional characterization, unveil new desferrioxamine traits. FEMS Microbiol Ecol. 2017;93. doi:10.1093/femsec/fix086

30. Bailey TL, Williams N, Misleh C, Li WW. MEME: discovering and analyzing DNA and protein sequence motifs. Nucleic Acids Res. 2006;34: W369-73. doi:10.1093/nar/gkl198

31. Grant SG, Jessee J, Bloom FR, Hanahan D. Differential plasmid rescue from transgenic mouse DNAs into Escherichia coli methylation-restriction mutants. Proc Natl Acad Sci

USA. 1990;87: 4645–4649.

32. Bi C, Su P, Müller J, Yeh Y-C, Chhabra SR, Beller HR, et al. Development of a broad-host synthetic biology toolbox for Ralstonia eutropha and its application to engineering hydrocarbon biofuel production. Microb Cell Fact. 2013;12: 107. doi:10.1186/1475-2859-12-107

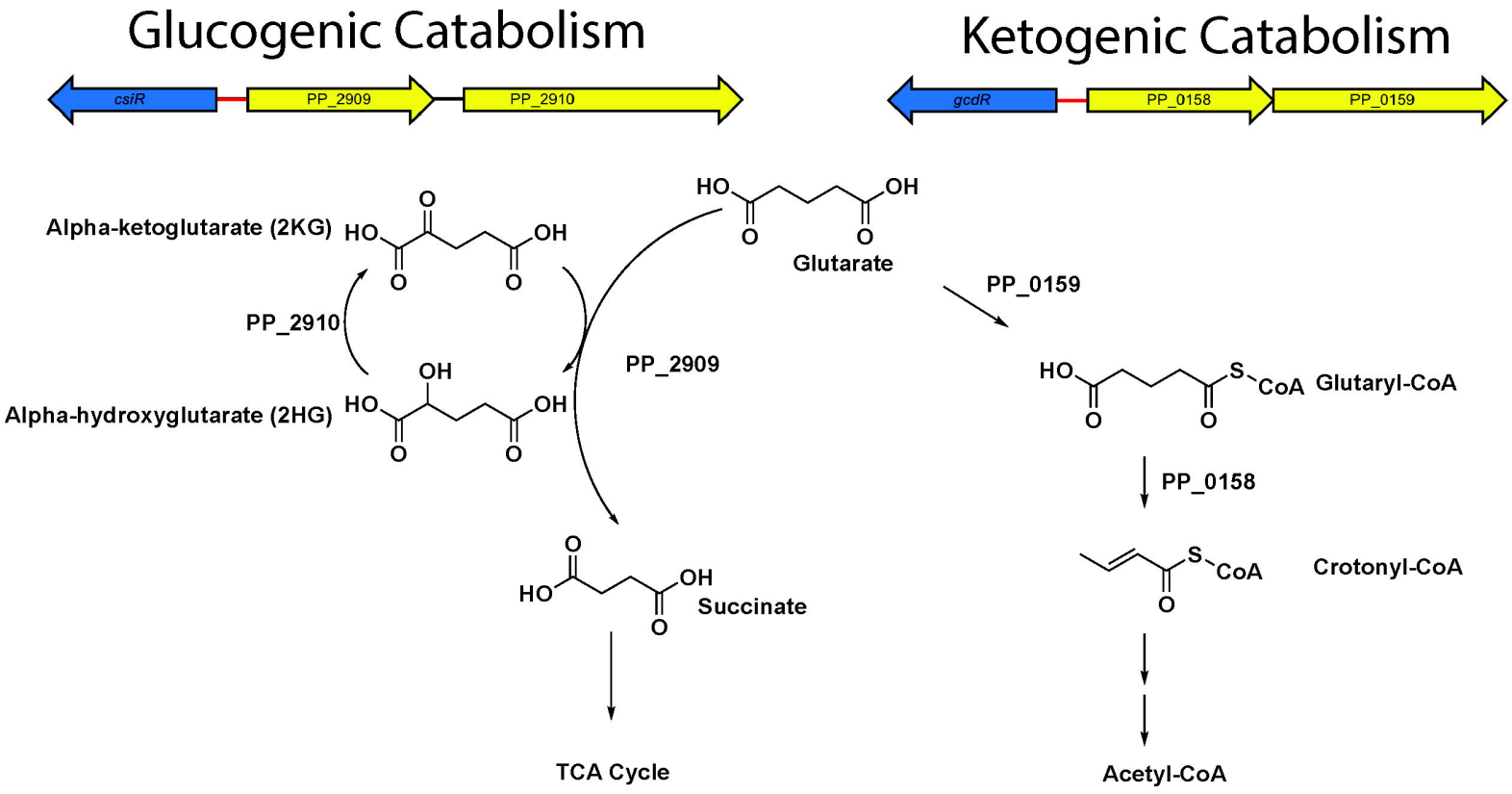
Glucogenic Catabolism
csiR
PP_2909
PP_2910
Ketogenic Catabolism
gcdR
PP_0158
PP_0159
Alpha-ketoglutarate (2KG)
Alpha-hydroxyglutarate (2HG)
PP_2910
PP_2909
Glutarate
PP_0159
Glutaryl-CoA
PP_0158
Crotonyl-CoA
Succinate
TCA Cycle
Acetyl-CoA

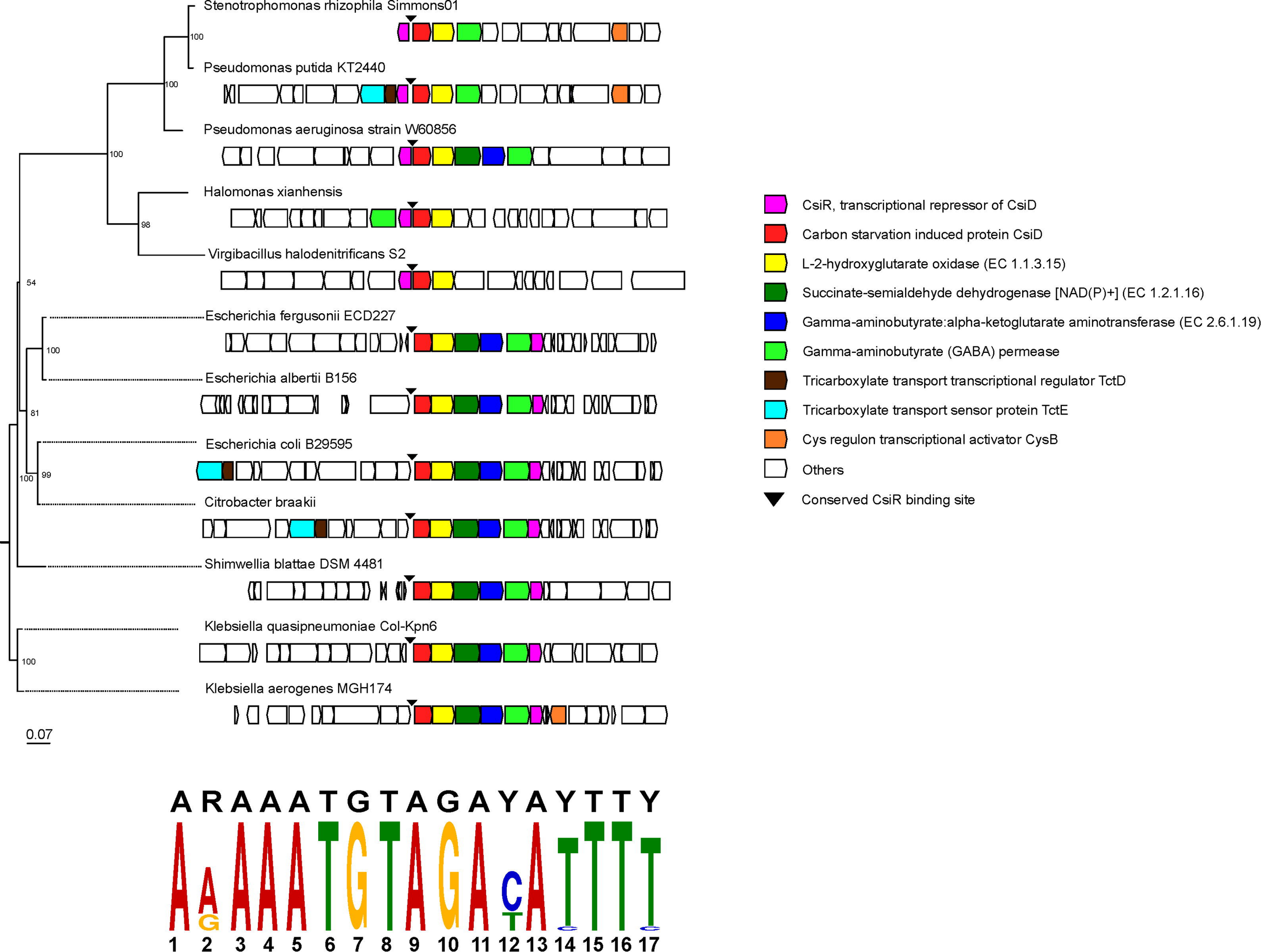
Stenotrophomonas rhizophila Simmons01
Pseudomonas putida KT2440
Pseudomonas aeruginosa strain W60856
Halomonas xianhensis
Virgibacillus halodenitrificans S2
Escherichia fergusonii ECD227
Escherichia albertii B156
Escherichia coli B29595
Citrobacter braakii
Shimwellia blattae DSM 4481
Klebsiella quasipneumoniae Col-Kpn6
Klebsiella aerogenes MGH174
100
100
100
98
54
100
81
100
99
100
0.07
CsiR, transcriptional repressor of CsiD
Carbon starvation induced protein CsiD
L-2-hydroxyglutarate oxidase (EC 1.1.3.15)
Succinate-semialdehyde dehydrogenase [NAD(P)+] (EC 1.2.1.16)
Gamma-aminobutyrate:alpha-ketoglutarate aminotransferase (EC 2.6.1.19)
Gamma-aminobutyrate (GABA) permease
Tricarboxylate transport transcriptional regulator TctD
Tricarboxylate transport sensor protein TctE
Cys regulon transcriptional activator CysB
Others
Conserved CsiR binding site
A R A A A T G T A G A Y A Y T T Y
1 2 3 4 5 6 7 8 9 10 11 12 13 14 15 16 17

A

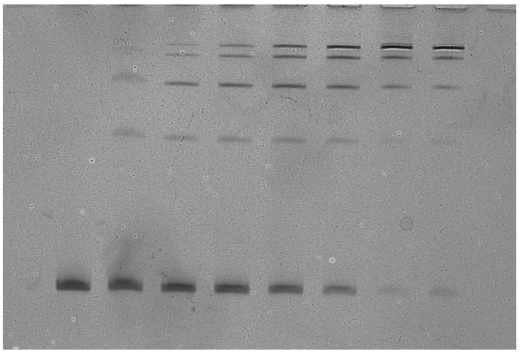

CsiR Concentration

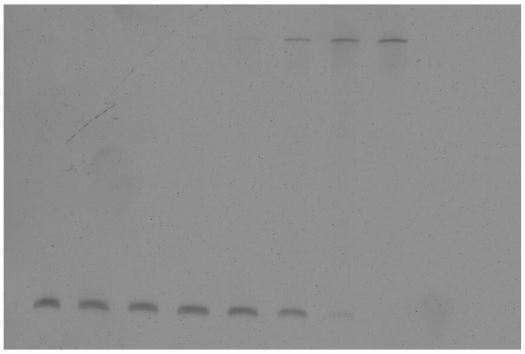

GcdR Concentration

B

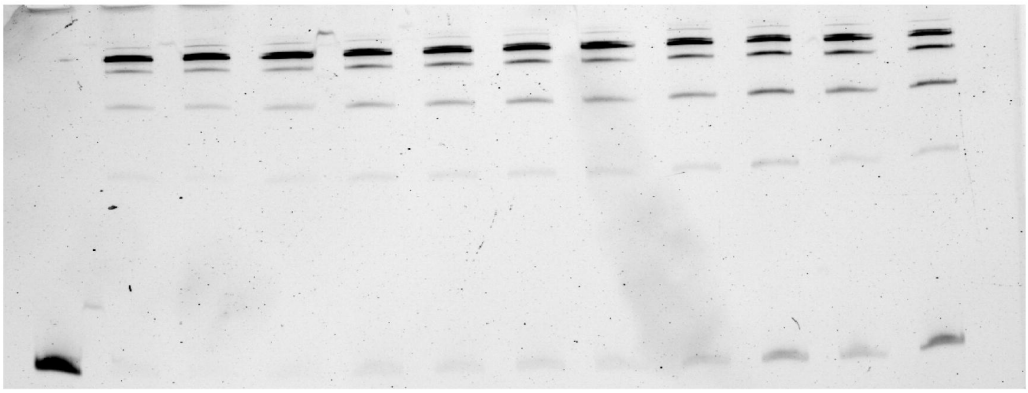

Glutarate Concentration

A

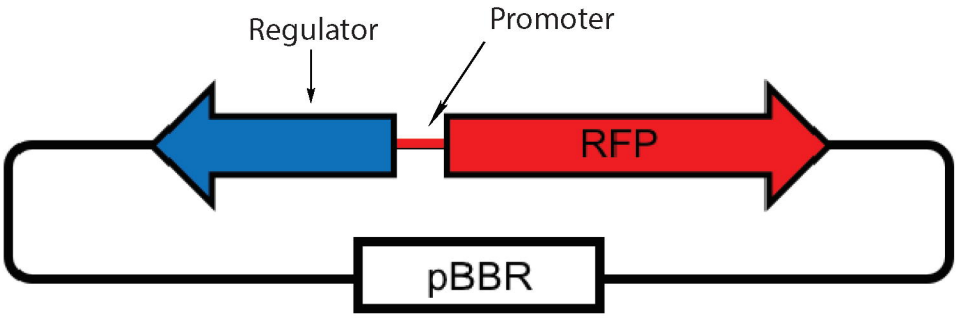

B

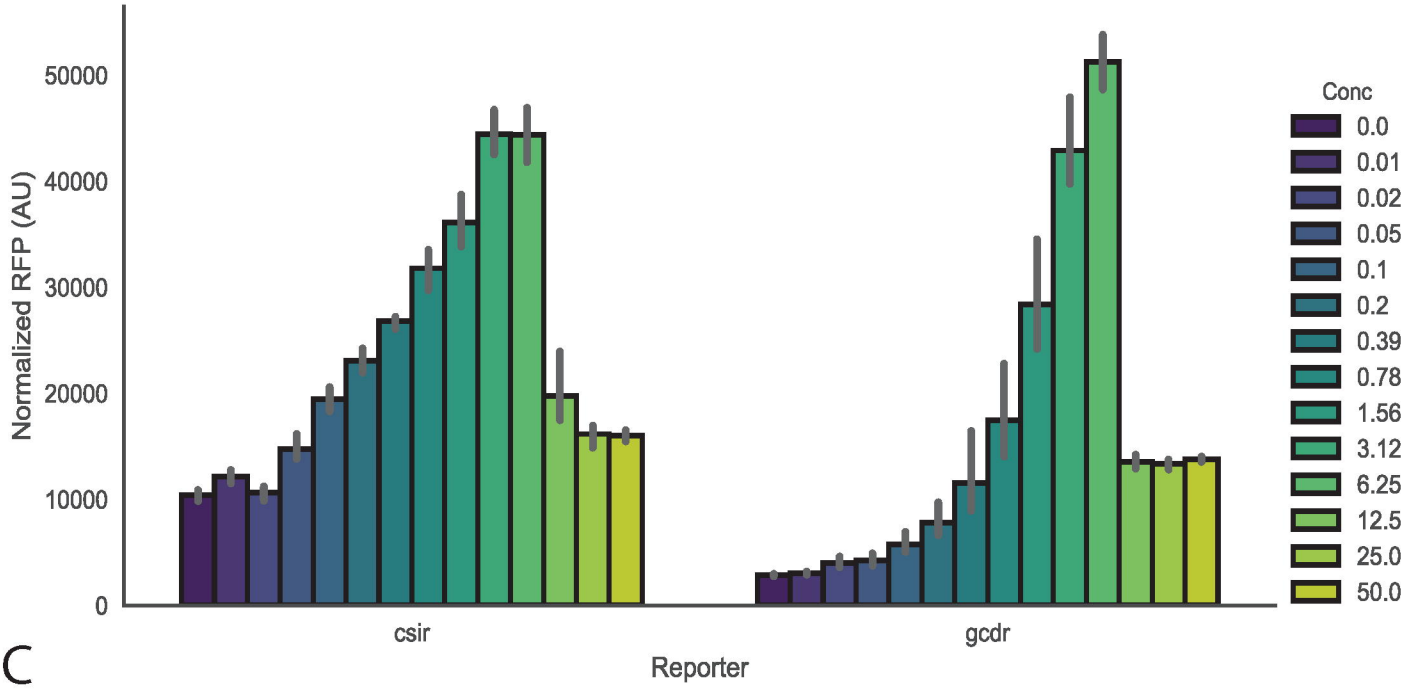

C

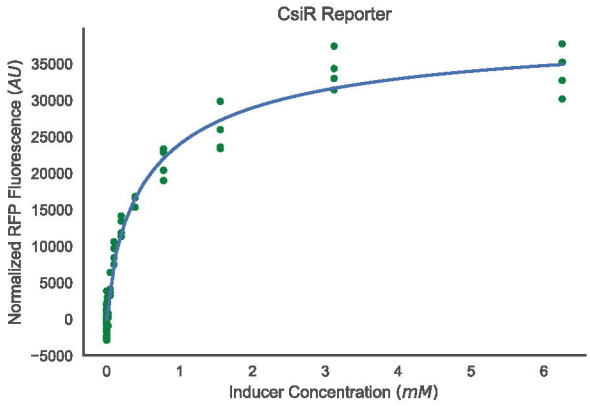

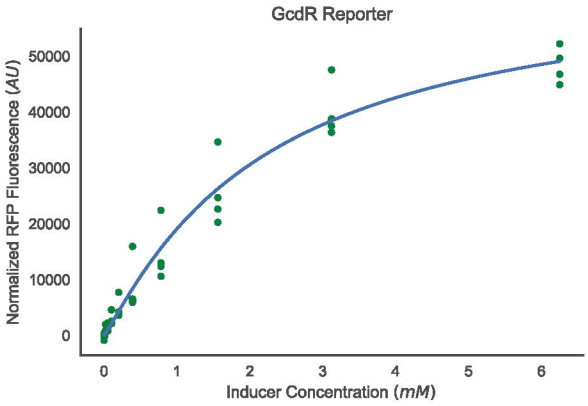

Sensor	RFPmax	Km (mM)	Hill Coefficient	Linear Range (mM)
CsiR	42000	0.65	0.75	0.05-3.13
GcdR	65000	2.24	1.09	0.05-6.25

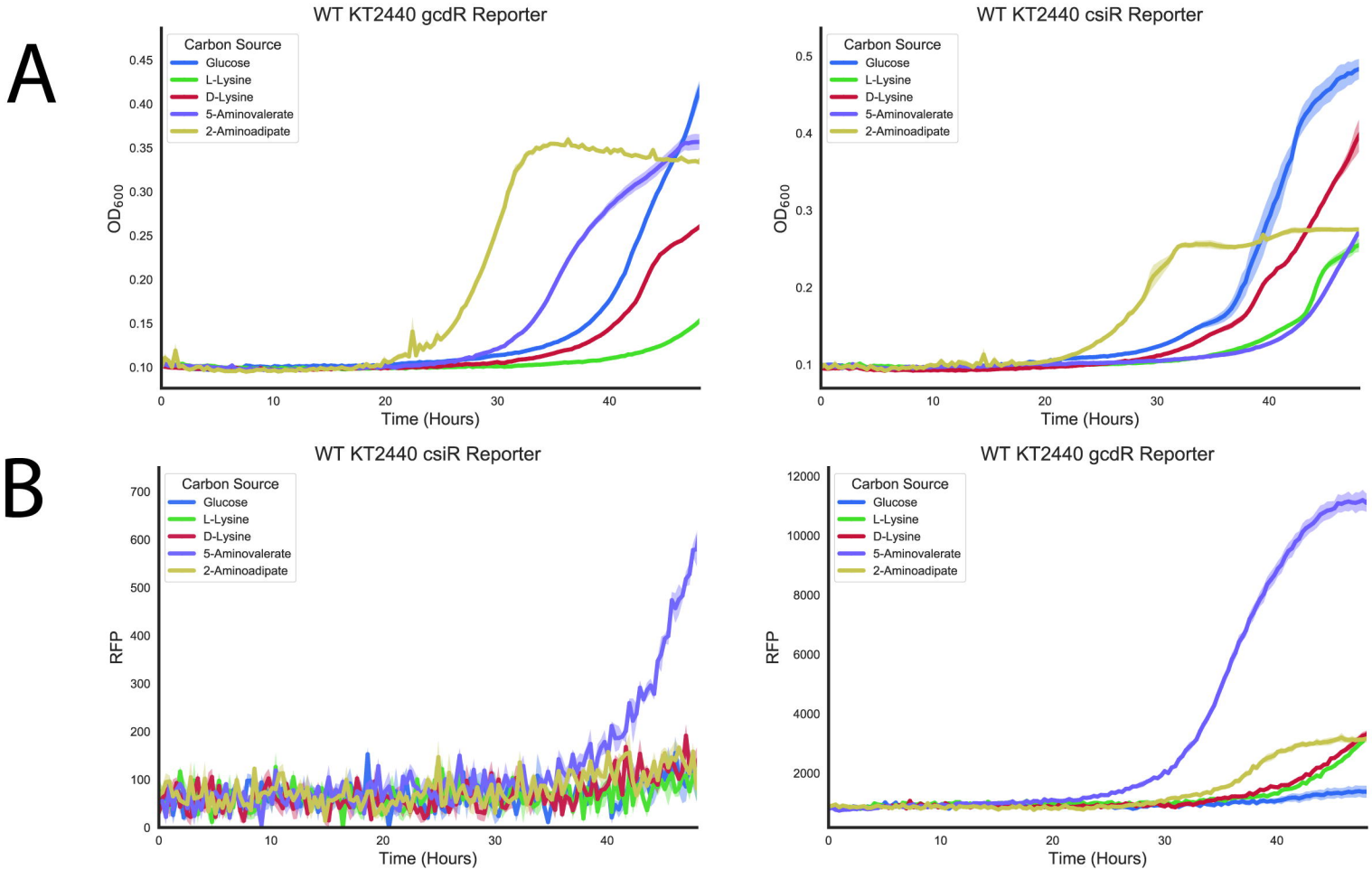
A
WT KT2440 gcdR Reporter
WT KT2440 csiR Reporter
Carbon Source
Glucose
L-Lysine
D-Lysine
5-Aminovalerate
2-Aminoadipate
OD600
Time (Hours)
B
WT KT2440 csiR Reporter
WT KT2440 gcdR Reporter
RFP
Time (Hours)